Actin Is Involved in Auxin-Dependent Patterning[1]

Jan Maisch* and Peter Nick

Institute of Botany 1, University of Karlsruhe, D–76128 Karlsruhe, Germany

Polar transport of auxin has been identified as a central element of pattern formation. The polarity of auxin transport is linked to the cycling of pin-formed proteins, a process that is related to actomyosin-dependent vesicle traffic. To get insight into the role of actin for auxin transport, we used patterned cell division to monitor the polarity of auxin fluxes. We show that cell division in the tobacco (*Nicotiana tabacum* L. cv Bright-Yellow 2) cell line is partially synchronized and that this synchrony can be perturbed by inhibition of auxin transport by 1-*N*-naphthylphthalamic acid. To address the role of actin in this synchrony, we induced a bundled configuration of actin by overexpressing mouse talin. The bundling of actin impairs the synchrony of cell division and increases the sensitivity to 1-*N*-naphthylphthalamic acid. Addition of the polarly transported auxins indole-3-acetic acid and 1-naphthyl acetic acid (but not 2,4-dichlorophenoxyacetic acid) restored both the normal organization of actin and the synchrony of cell division. This study suggests that auxin controls its own transport by changing the state of actin filaments.

The promotion of growth and signaling from both developmental programs and environmental stimuli are often mediated by auxin, one of the major plant hormones. In addition, auxin is involved in directional cues fundamental to patterning (for review, see Berleth and Sachs, 2001). Classical examples for auxin-dependent patterning have been the formation of leaf veins (Mattsson et al., 1999), the positioning of meristems (Reinhard et al., 2000), and the organization of vascular tissue (Sachs, 2000).

The cellular base of auxin-dependent patterning is related to the establishment of a directional flow. This polar transport of auxin is a cell-to-cell process that has been described in a modified chemiosmotic model for auxin transport (for review, see Lomax et al., 1995).

This implies that patterning is brought about by communication between cells that exchange morphogenetic signals in a defined direction. In other words, patterning is driven by cell polarity. Therefore, synchrony and coordination between neighboring cells are of extreme importance for the development of a functional tissue (Sachs, 1993).

The self amplification of cell polarity by a polar auxin flow has been linked with directional intracellular traffic that contains positive feedback loops in combination with lateral inhibition, resulting in an ordered pattern (for review, see Nick, 2006). This mechanism has been elegantly demonstrated for the venation in developing leaves (Sachs, 2000), leading to the auxin-canalization model.

Several experiments demonstrated the central role of basipetal auxin transport in mediating this directionality, mainly by means of the polarized activity of auxin efflux carriers (for review, see Morris, 2000; Blakeslee et al., 2005; Leyser, 2006). In the meantime, several pin-formed (PIN) proteins have been identified as candidates for auxin efflux facilitator proteins (for review, see Chen and Masson, 2006), and despite a long debate on the actual function of these proteins, the most recent results show that they are in fact rate limiting for auxin efflux (Petrášek et al., 2006). In general, vesicular trafficking regulated by ADP-ribosylation factors and ADP-ribosylation factor guanine nucleotide exchange factors appears to be involved in the recycling of various PIN proteins between the plasma membrane and endosomal compartments (Geldner et al., 2003).

When plant samples are treated with brefeldin A (BFA) that selectively blocks secretory pathways from endosomes to the plasma membrane, the plasma membrane-localized PIN1 protein is trapped in intracellular compartments (Steinmann et al., 1999; Geldner et al., 2001). This reversible effect of BFA on PIN1 internalization and cycling is interrupted in the presence of the actin depolymerization drug cytochalasin D, indicating that the endosomal exocytosis of PIN1 is actin dependent. Moreover, this cycling is also regulated by auxin (Paciorek et al., 2005).

A link between actin and auxin signaling has also been proposed from studies on auxin-dependent cell growth in Graminean coleoptiles. In this model, an auxin-dependent reorganization of actin filaments into fine cortical strands could be shown to correlate with the auxin response of growth (Waller et al., 2002). By transient transformation with the actin-binding domain of mouse talin (mT) in a fusion with a fluorescent

[1] This work was supported by the Landesgraduierten-Programm of the State of Baden-Württemberg (fellowship to J.M.), and by the Landesschwerpunkt-Programm of the State of Baden-Württemberg (LuNaCell; to P.N.).

* Corresponding author; e-mail jan.maisch@botanik1.uni-karlsruhe.de; fax 49–721–608–4193.

The author responsible for distribution of materials integral to the findings presented in this article in accordance with the policy described in the Instructions for Authors (www.plantphysiol.org) is: Jan Maisch (jan.maisch@botanik1.uni-karlsruhe.de).

www.plantphysiol.org/cgi/doi/10.1104/pp.106.094052

protein, it became possible to follow the loosening of actin filaments in living rice (*Oryza sativa*) coleoptiles (Holweg et al., 2004). Upon treatment with BFA, actin became trapped on the endomembrane system and was partitioned into the microsomal fraction. The cellular correlate of this trapping was a bundling of cortical actin strands into dense bundles. This was accompanied by a shift of the dose response of auxin-dependent cell elongation toward higher concentrations. Thus, a bundling of actin resulted in a reduction of auxin-sensitivity in sensu strictu. These observations linked auxin signaling, vesicle flow, and the organization of actin filaments. The causal relationship between these three events remained unresolved.

The actin cytoskeleton has also been implicated in regulating gravitropism, because interruption of intact actin filaments by the actin depolymerization drug latrunculin B enhances the gravitropic responses in different plant species (Hou et al., 2004). The effect of latrunculin B impairs the fine meshwork of actin filaments in different regions of the treated roots, alters the dynamics of amyloplast sedimentation in the columella cells, and prolongs the intracellular alkalinization response. These abnormalities are accompanied by a persistent auxin gradient in the root cap.

In general, an intact actin cytoskeleton is required for functional auxin responses. Because the organization of actin in turn depends on auxin, this constitutes a self-amplification loop between auxin signaling and actin filaments (for review, see Nick, 2006). To demonstrate this loop directly, it is necessary to dissect and manipulate individual elements in this nonlinear, self-referring system.

In a previous work, we used patterned cell division in tobacco (*Nicotiana tabacum*) L. cv Virginia Bright Italia 0 (VBI-0) cells to monitor the polarity of auxin fluxes (Campanoni et al., 2003). In this tobacco line, cell division followed a clear pattern with elevated frequencies of files composed of an even number of cells. This type of division pattern resulted from weak coupling between the divisions of neighboring cells. The coupling was dependent on polar auxin flux and displayed a clear unidirectionality. Because VBI-0 derives from a specific tissue (stem pith parenchyma) this pattern might represent a peculiar feature of this cell line. Because VBI-0 was found to be recalcitrant to stable transformation, we asked whether patterning can be analyzed in the widely used Bright-Yellow 2 (BY-2), where a panel of numerous fluorescent marker lines is available.

The use of the model tobacco BY-2 has generated a wealth of data on the role of phytohormones during the plant cell cycle (Nagata et al., 1992). The possibility to synchronize BY-2 (Nagata et al., 1992; Nagata and Kumagai, 1999) provided a powerful approach to detect fluctuations of hormone levels during cell division (Redig et al., 1996). The BY-2 cell line is characterized by well-defined axial cell divisions that generate pluricellular, polar cell files exhibiting basic features of pattern formation. Further, the directional flow of auxin within cell files can be inhibited in this cell line by 1-*N*-naphthylphthalamic acid (NPA) at conditions that do not affect the structure of the cytoskeleton (Petrášek et al., 2003).

The BY-2 cell line grows in simple files that exhibit basic characteristics of pattern formation, such as clear axis and polarity of cell division and growth. Therefore, this system is well suited to study spatial aspects of cell division. In fact, it could be shown that high concentrations of NPA perturb the axiality of cell division. For instance, the formation of preprophase bands was abnormal, leading to disoriented, oblique cell plates and malformed cells (Dhonukshe et al., 2005). However, to our knowledge, these cells have not been analyzed with respect to supracellular patterning and the role of auxin and actin therein. In this work, we use BY-2 as a model system to study intracellular communication in patterning. We show that cell division within cell files is partially synchronized, leading to higher frequencies of files with even cell numbers as compared to files with uneven cell numbers. By inhibiting the polar auxin flux using low concentrations of NPA, we demonstrate that the pattern of cell division within BY-2 cell files depends on auxin. Based on these properties, we ventured to address the role of actin in auxin signaling using patterning as sensitive trait to monitor changes of polar auxin fluxes. If actin is part of an auxin-driven feedback loop, it should be possible to manipulate auxin-dependent patterning through manipulation of actin.

To test this prediction, we used a transgenic BY-2 cell line stably expressing a fusion between the yellow fluorescent protein (YFP) and the actin-binding domain of mT. In this cell line, the actin filaments are constitutively bundled, and the synchrony of cell division is impaired in such a way that the pattern of cell division is affected. When we added polar transportable auxins (but not auxin per se), both a normal organization of actin and the synchrony of cell division could be restored. We therefore conclude that actin is not only responsive to changes in the cellular content of auxin but also that the organization of actin filaments is crucial for auxin transport. This indicates a regulatory mechanism by which auxin controls its own transport through changing the organization of actin filaments.

RESULTS

Cell Division within Cell Files of BY-2 Is Synchronized by a NPA-Sensitive Signal

To assess cell division patterns, we first had to define the onset of the stationary phase. We therefore followed the time course of cell division in nontransformed BY-2 cells and in BY-2 cells overexpressing YFP-mT. Although cell division activity in the YFP-mT line was delayed by about 0.5 to 1 d and reduced in amplitude, the temporal pattern was very similar, and

cell density approached a plateau from 4 d after subcultivation (Fig. 1A). We therefore constructed at this time point frequency distributions over the cell number per individual file.

Under standard cultivation conditions, the frequency distribution of nontransformed BY-2 cells exhibited characteristic peaks of frequency for files composed of two, four, and six cells (Fig. 1B). Similar distributions were observed throughout the entire exponential phase (data not shown). Thus, files with even cell numbers are more frequent than files with uneven cell numbers.

In the next step, we asked whether this characteristic pattern was related to auxin transport. Therefore, BY-2 cells were inoculated in presence of 3 or 12 μM NPA, an inhibitor of polar auxin transport. The concentrations were chosen such that neither polarity nor axiality of cell files nor their viability were affected (data not shown). What was affected under these conditions was the distribution of cell division (Fig. 1, C and D). Treatment with these low concentrations of NPA progressively equalized the frequencies of files with even and uneven cell numbers, especially for files with a higher number of cells. It should be noted that, at 3 μM NPA, cell division (Fig. 1, F1 and F2) was only slightly reduced and cell elongation (Fig. 1G) was not affected at all. From 12 μM NPA, the inhibition of cell division became evident (Fig. 1, F1 and F2), and cell elongation increased progressively (Fig. 1G1). However, for a high concentration (30 μM) of NPA, the upper two frequency peaks disappeared (Fig. 1E), and files with more than four cells became very rare. Under these conditions, we observed a strong inhibition of cell division (Fig. 1, F1 and F2) and a significant stimulation of cell elongation (Fig. 1G1) that were accompanied by a loss of file polarity and axiality. Although the cells significantly increased in length, they exhibited localized swellings, resulting in irregular, bulbous cell shapes (Fig. 1G2). In addition, the difference between the more pointed terminal cells of a file and the more isodiametric cells in the center of a file vanished progressively. We tested whether the loss of synchrony was limited to NPA or whether it could be induced by other inhibitors of polar auxin flow. We therefore tested the effect of 12 μM 2,3,5-triiodobenzoic acid (TIBA) and observed that, similar to NPA, the synchrony of cell division was lost such that the difference in frequency between even and uneven cell numbers disappeared (Fig. 5A). To test whether the observed loss of synchrony might be caused by a precocious and randomized disintegration of cell files, we calculated the mean number of cells per file as indicator. For 3 μM of NPA, where synchrony was already conspicuously affected (Fig. 1C), this indicator was almost identical with that of untreated control cells (3.91 versus 4.09). Thus, the reduced synchrony is not due to premature disintegration. We also recorded the possible influence of aberrant cell divisions (oblique or longitudinal). These were occasionally observed, but at such a rare frequency that there was no statistically measurable effect on the frequency distributions (data not shown).

Because NPA blocks auxin efflux and causes accumulation of auxin within cells, the actual effect might be an accumulation of auxin due to reduced efflux. If this idea is correct, one would predict that a mild treatment with NPA combined with addition of low concentrations of the polar transportable auxin indole-3-acetic acid (IAA) in nontransformed cells should phenocopy the effect of a high concentration of NPA. We therefore tested what happened when nontransformed cells were treated by a combination of a low (3 μM) concentration of NPA with a low (2 μM) concentration of IAA. We observed that this resulted in a conspicuous loss of division synchrony mimicking the effect of a high (12 μM) concentration of NPA (Fig. 5B).

These data show that, in this cell line, the pattern of cell division depends on polar auxin flow within the cell file (despite the overall presence of 0.9 μM of the artificial auxin 2,4-dichlorophenoxyacetic acid [2,4-D] in the medium). The synergistic effect of low concentrations of NPA with low concentrations of IAA indicates that it is the intracellular accumulation of IAA that is responsible for the reduced synchrony in response to the phytotropin NPA.

Actin Is Constitutively Bundled in a BY-2 Line Overexpressing YFP-mT

To better understand the role of actin in auxin-dependent patterning, we searched for a situation where actin filaments were constitutively bundled. For this purpose, we generated a transgenic BY-2 cell line stably transformed with a fusion between YFP and the actin-binding domain of mT under control of a 35S promoter. We wanted to test whether the excess of YFP-mT fusion would cause a constitutive bundling of actin filaments. If so, it should be possible, by means of the YFP-mT line, to manipulate auxin-dependent patterning through the altered organization of actin in this cell line. Therefore, we compared the arrangement of actin filaments in nontransformed control cells with cells overexpressing YFP-mT (Figs. 2 and 3). The actin cytoskeleton was visualized either in nontransformed BY-2 cells by the rhodamine-phalloidin staining method or, in the case of the BY-2 YFP-mT line, observed directly in vivo.

To confirm that YFP-mT binds to and visualizes actin filaments, BY-2 cells overexpressing the fusion protein were also costained with rhodamine-phalloidin. Patterns of yellow YFP-fluorescence and red rhodamine-phalloidin fluorescence emitted from double-labeled BY-2 cells were essentially identical (Fig. 2), showing that YFP-mT binds to the entire actin cytoskeleton in a specific manner.

The nontransformed BY-2 cells displayed a fine network of transversely oriented actin filaments in the cortical region (Fig. 3A). Prominent fine actin filaments were also visible around the nucleus and radially oriented in transvacuolar strands (Fig. 3B). In contrast, actin was heavily bundled in cells overexpressing YFP-mT both in the cortical (Fig. 3E) and in

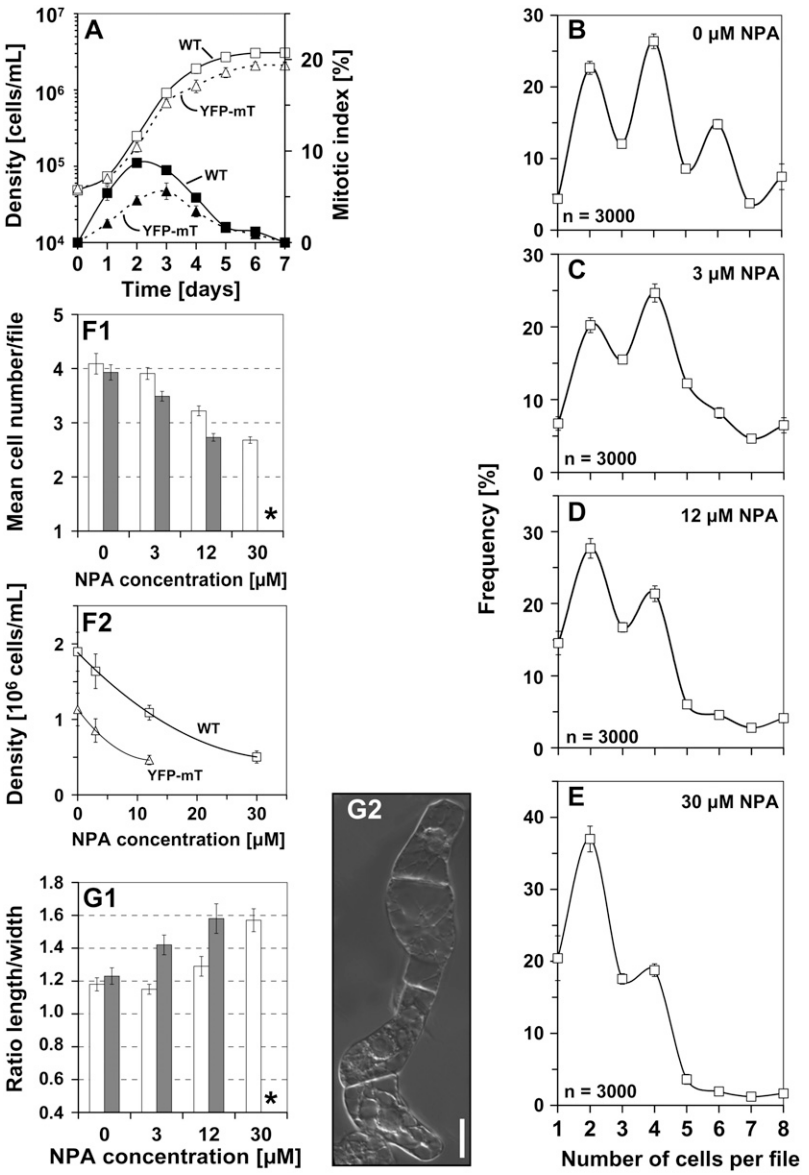

Figure 1. Cell division in nontransformed BY-2 cells follows a pattern that depends on polar auxin fluxes. A, Cell density (white symbols) and mitotic indices (black symbols) over time after subcultivation of nontransformed BY-2 cells (wild type, squares, solid curves) and BY-2 cells overexpressing YFP-mT (triangles, dotted curves). Each point represents the mean from 1,000 scored cells. B to E, Frequency distribution over cell number per file in nontransformed BY-2 cells at day 4 after inoculation in the absence of NPA (B) or in presence of 3 (C), 12 (D), or 30 (E) μM NPA. Error bars indicate SE. F and G, Effect of NPA on cell division (F1, F2) and cell elongation (G1) in nontransformed BY-2 cells (white bars) versus cells overexpressing YFP-mT (black bars) at day 4 after inoculation. Each distribution is based on 3,000 individual cells from three independent experimental series. Cell division is plotted as mean number of cells per file (F1) and as cell density (F2) and cell elongation as ratio of cell length over cell width (G1). Error bars indicate SE. Asterisks, YFP-mT cells died at 30 μM NPA such that a measurement of length to width ratio was not meaningful. G2, Morphology of nontransformed BY-2 cells after treatment with 30 μM NPA. Bar = 20 μm.

the perinuclear regions (Fig. 3F). These observations demonstrate that the overexpression of the actin-binding domain of mT indeed induced a strong reorganization of the actin cytoskeleton.

The Synchrony of Cell Division Is Affected by Bundling of Actin

With exception of a small delay and a somewhat reduced amplitude of the division response, the global temporal pattern of cell division in the YFP-mT line was comparable to that in the nontransformed BY-2 cell line (Fig. 1A). However, the synchrony of cell division was affected in the YFP-mT line (Fig. 4A). The characteristic oscillatory behavior typical for the nontransformed control is hardly detectable. In other words, the difference in the incidence of files with even and uneven cell numbers is strongly reduced in YFP-mT cells. This difference was persistent when the selective pressure on the cell line was relieved by omitting hygromycin from the medium, suggesting that it is an effect of the transgene and not an effect of the selection pressure. The average number of cells per file as indicator for a possible precocious disintegration of files did not reveal significant differences to the nontransformed wild type (3.93 versus 4.09, respectively). Thus, the reduced synchrony in the YFP-mT line is not due to a premature disintegration of cell files. We also scored for the possible influence of aberrant cell divisions but were not able to detect any statistically measurable effect on synchrony.

We further investigated how the pattern of cell division responded to treatment with NPA. Similar to the nontransformed BY-2 cell line, the frequency

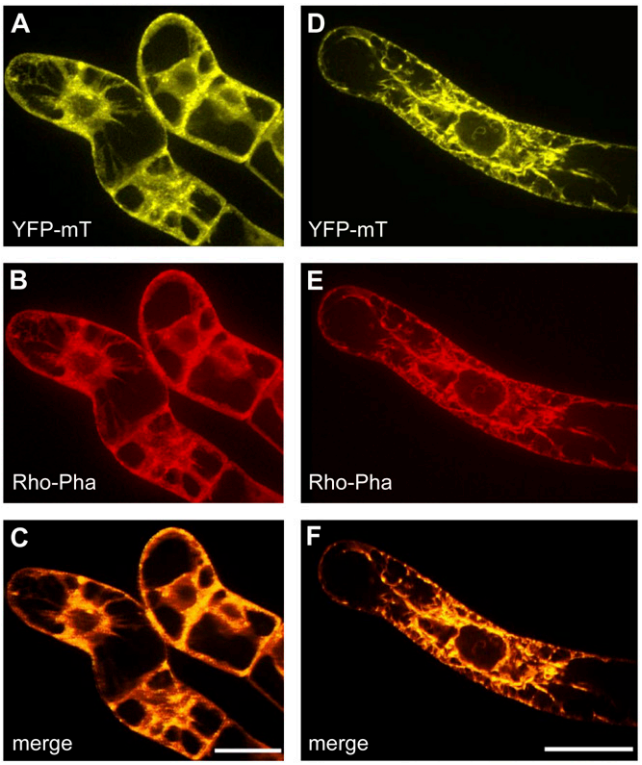

Figure 2. Colocalization of YFP-mT and of rhodamine-phalloidin in BY-2 cells overexpressing YFP-mT in the absence (A–C) or in presence (D–F) of 2 μM IAA. YFP-mT fluorescence (A and D). Rhodamine-phalloidin fluorescence (B and E). C and F, Merged fluorescences of A and B or D and E, respectively. Orange color indicates areas where the images overlap and where the two markers colocalize. Bars = 20 μm.

peaks for higher cell numbers disappeared progressively (Fig. 4, B and C). Generally, the YFP-mT cell line appeared to be affected more readily compared to the nontransformed cell line. Already, for 12 μM, NPA files with more than two cells had become very rare (Fig. 4C), whereas in the nontransformed cell line, a higher concentration (30 μM NPA) was required to cause a similar effect (Fig. 1E). Conversely, the effect of 3 μM NPA in the YFP-mT cell line was comparable to that observed in the nontransformed cell line upon addition of 12 μM NPA. Moreover, cell division was more impaired (Fig. 1, F1 and F2), and cell elongation was more elevated (Fig. 1G1) at 12 μM NPA in the YFP-mT cell line compared to the nontransformed cell line. Because viability at 30 μM NPA was strongly reduced in the YFP-mT cell line (in contrast to the nontransformed cell line), it was not possible to measure cell division responses for the transgenic line (data not shown). In summary, already low concentrations of NPA caused effects in the YFP-mT cell line that were observed in the nontransformed cell line only for higher concentrations of this inhibitor. In other words, the YFP-mT line is, in sensu strictu, more sensitive to NPA compared to the nontransformed BY-2 cell line.

These data show that the synchrony of cell division is already a priori strongly deteriorated compared to the nontransformed cell line. This is accompanied by an elevated sensitivity of cell division to NPA. Thus, the constitutive bundling of actin filaments in the YFP-mT line was accompanied by impaired synchrony in auxin-dependent patterning.

The Synchrony of Cell Division Can Be Restored by Polar Transportable Auxins

If the observed correlation between constitutively bundled actin and impaired synchrony of cell division is the manifestation of a causal relationship, we would predict that synchrony should be restored when the microfilament bundles are replaced by a configuration with finer, detached actin filaments. To test this prediction, we tried to generate detached microfilament strands by addition of supplementary auxins. The BY-2 cells overexpressing YFP-talin were cultivated either upon addition of the auxins IAA or 1-naphthyl acetic acid (NAA) that are both polarly transported or the

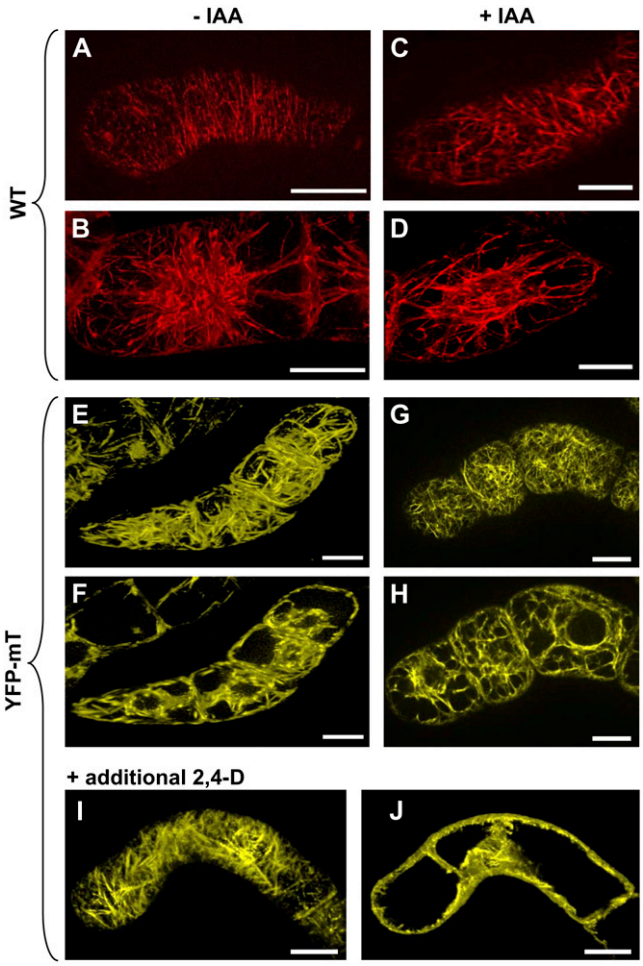

Figure 3. Actin filaments in nontransformed BY-2 cells (wild type, A–D) visualized by TRITC-phalloidin in comparison with cells overexpressing YFP-mT (E–J) in the absence (A, B, E, and F) and the presence (C, D, G, and H) of 2 μM IAA or in the presence of additional 2 μM 2,4-D (I and J). For each cell, a focal section in the cortical (A, C, E, G, and I) and in the central (B, D, F, H, and J) region is shown. Bars = 20 μm.

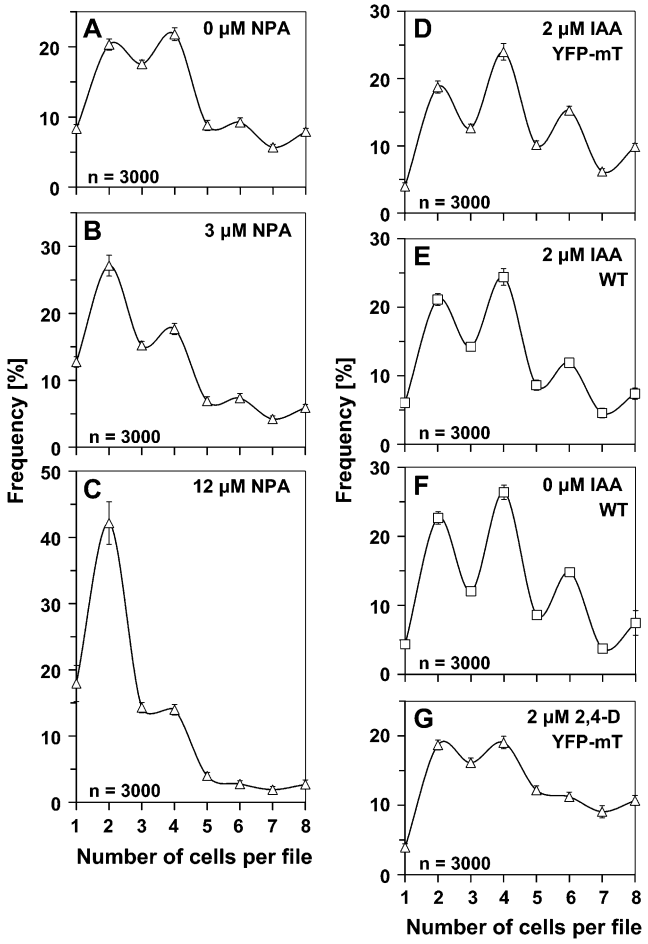

Figure 4. Frequency distribution over cell number per file in BY-2 cells overexpressing YFP-mT at day 4 after inoculation in the absence of NPA (A), in the presence of 3 (B) or 12 μM NPA (C), or upon supplementation with 2 μM IAA (D) or additional 2 μM 2,4-D (G). As a control, the response of nontransformed (wild type) cells to 2 μM IAA (E) is shown in comparison to the distribution in the absence of IAA (F). Each distribution is based on 3,000 individual cells from three independent experimental series. Error bars indicate SE.

same concentration of 2,4-D, an auxin that, at least in BY-2 cells, was not a good substrate for the efflux carrier responsible for polar auxin flow (Delbarre et al., 1996; Paciorek et al., 2005).

The presence of IAA leads to a debundling of actin both in the cortical region and around the nucleus. In contrast to the massive actin bundles characteristic for the IAA-free sample (Fig. 3, E and F), numerous fine cortical actin filaments were observed upon addition of 2 μM IAA (Fig. 3G) and even the transvacuolar strands were much finer than in the untreated control (Fig. 3H). This auxin effect was specific for IAA when 2 μM 2,4-D was added (in addition to the 0.9 μM corresponding to 0.2 mg/L of 2,4-D that was present in all samples); this had no effect on the arrangement of actin filaments (Fig. 3, I and J).

How did these hormone treatments affect the pattern of cell division in the YFP-mT line? After addition of IAA, the synchrony of cell division, manifest as the characteristic pattern with elevated frequencies of even-numbered cell files, was restored in the YFP-mT cell line (Fig. 4D). In contrast, additional 2,4-D just shifted the frequency distribution toward higher cell numbers without restoring synchrony; the residual difference in the frequencies of even and uneven cell numbers was even lower than in the untreated control line (compare Fig. 4, G to A). When we tested the response of nontransformed control cells to IAA, we did not see any significant change of synchrony. The only effect consists of a slight shift of the distribution to higher cell numbers (compare Fig. 4, E to F). A treatment with 2 μM NAA, in contrast, was able to rescue the synchrony of cell division partially (Fig. 5C). However, NAA was clearly less effective than IAA.

Summarizing these results, we observed that actin was constitutively bundled in a BY-2 line overexpressing YFP-mT. This bundling of actin interferes with the synchrony of cell division in such a way that the division pattern is affected. Addition of polarly transported auxins, but not an increase of auxin per se, could restore both a normal organization of actin and the synchrony of cell division.

DISCUSSION

Cell divisions were also synchronized in BY-2 cells. We observed a clear pattern of cell division consisting of elevated frequencies of even-numbered cell files (Fig. 1B). We further observed that a mild inhibition of polar auxin transport, which only slightly affects the rate of cell division (Fig. 1, F1 and F2) and leaves cell elongation unaffected (Fig. 1G1), equalizes the prevalence of files with even cell numbers (Fig. 1C). This effect is induced by not only NPA, but also by other phytotropins (such as TIBA; Fig. 5A). The actual signal seems to be the intracellular accumulation of IAA produced by these phytotropins. We conclude this from the synergistic effect of low concentrations of IAA with low concentrations of NPA (Fig. 5B). We conclude that, in BY-2 as well, polar intrafile auxin transport and not auxin per se is responsible for the patterning of cell division.

These experiments confirmed that BY-2 is a suitable system to study auxin-dependent patterning of cell division. In the next step, we asked for the role of actin in the generation of this pattern. Our previous work has shown that the auxin response to actin involves changes in the bundling of actin filaments, with bundled actin being characteristic for a situation where auxin was depleted (Waller et al., 2002; Holweg et al., 2004). These changes of actin organization feed back to the sensing and/or processing of auxin (Waller et al., 2002; Nick, 2006). We therefore searched for approaches to manipulate the bundling of actin filaments.

Although the expression of fluorescent proteins fused to actin-binding domains has been used as a

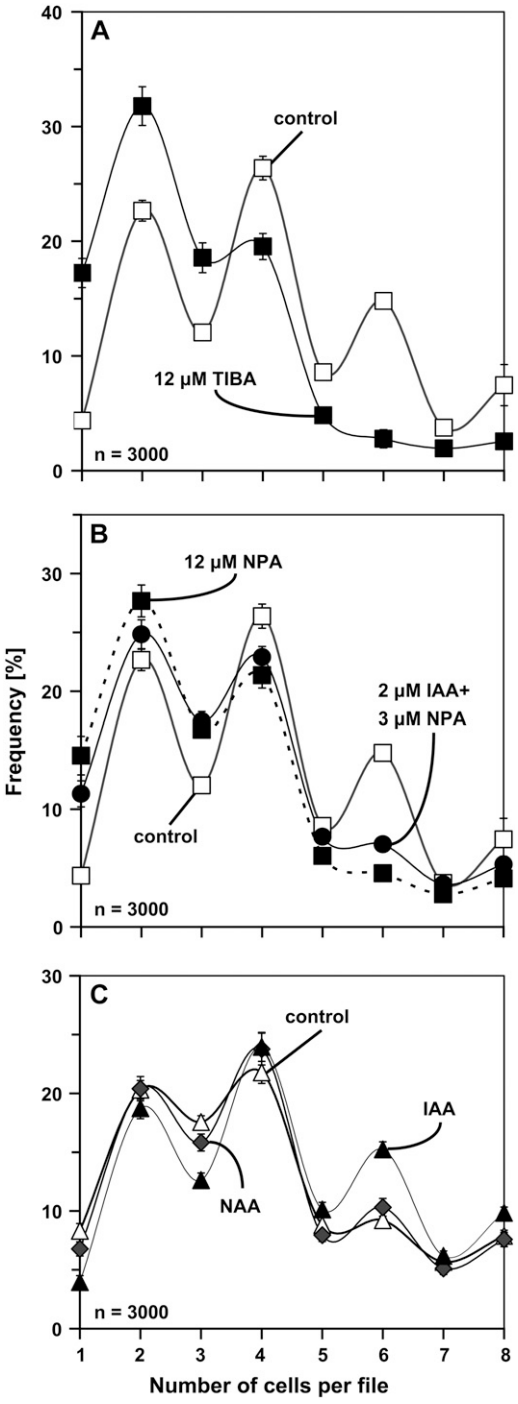

Figure 5. Manipulation of synchrony by 12 μM TIBA (compared to the untreated sample; A), a combined treatment with 3 μM NPA and 2 μM IAA (compared to the effect of 12 μM NPA and the untreated sample; B), and 2 μM NAA (compared to the effect of 2 μM IAA and the untreated sample; C). Frequency distribution over cell number per file is shown for nontransformed BY-2 cells (A and B) and BY-2 cells overexpressing YFP-mT (C) at day 4 after inoculation. Each distribution is based on 3,000 individual cells from three independent experimental series. Error bars indicate SE.

convenient tool to study the actin cytoskeleton in living cells, the dynamics and organization of F-actin may change due to the expression of the fusion protein. These changes may cause problems with transport or signaling processes affecting cell division and cell growth. As published by Ketelaar et al. (2004), the overexpression of mT can impair actin dynamics to some degree by inhibiting the actin-depolymerizing activity of actin-depolymerizing factor, resulting in a bundling of actin filaments. We therefore used mT overexpression to induce a constitutive bundling of actin filaments, thus mimicking a situation usually observed upon auxin depletion.

For this purpose, we used a transgenic BY-2 cell line overexpressing YFP-mT under control of the 35S promoter. To eliminate transformants with low expression activity, we applied a stringent selection regime. This resulted in a generally high level of expression leading to a very strong bundling of actin filaments (Fig. 3, E and F). This bundling was also shown by Kost et al. (1998) in growing tobacco pollen tubes using high expression levels of GFP-mT. When actin was visualized by rhodamine-phalloidin in the cells expressing YFP-mT, both signals were found to be congruent (Fig. 2). We are thus not able to detect any pool of F-actin that is not bundled or not properly visualized by YFP-mT.

We were now able to show that the bundling of actin interferes with the auxin-dependent synchrony of cell division. As a consequence of the impaired coordination of the cell cycle, the difference in the incidence of files with even and uneven cell numbers was strongly reduced already in untreated YFP-mT cells (Fig. 4A), an effect that could even be enhanced by treatment with NPA, an inhibitor of polar auxin flux. Already low concentrations of NPA produced alterations in the frequency distribution that were observed in the nontransformed cell line only for higher concentrations of this inhibitor. For instance, already for 12 μM NPA, files with more than two cells had become very rare. In the nontransformed cell line, a higher concentration (30 μM NPA) was required to cause a similar effect (compare Fig. 4C to 1E). In other words, the NPA sensitivity was increased in the YFP-mT line. This was also evident when overall division activity was plotted over the concentration of NPA (Fig. 1, F1 and F2).

Given the impact of actin filaments in cell division, the overexpression of YFP-mT might impair cell division as such. This might explain the slightly delayed growth of the YFP-mT line (Fig. 1A). However, NPA and YFP-mT have a multiplicative effect on the interference of the coupling signal, indicating that both factors target to the same signaling cascade. Thus, most certainly, the increased sensitivity to NPA in the YFP-mT line implies that the link between actin organization and synchrony of cell division is based on changes of the directional transport of auxin.

If this reasoning is correct, and the constitutively bundled actin as well as the impaired synchrony of cell division depends on polar auxin transport, this

synchrony should be restored when the massive actin bundles in the YFP-mT line are replaced by a finer meshwork of detached microfilament strands. We have tested this prediction experimentally by supplementing the medium either with polarly transported auxins (IAA and NAA) or 2,4-D that is not excreted by the efflux carrier responsible for polar auxin flux (Delbarre et al., 1996) to generate detached microfilament strands. Consistent with previous studies of maize (*Zea mays*) and rice coleoptiles (Waller et al., 2002; Holweg et al., 2004), we were able to demonstrate that IAA (but not 2,4-D) induced a dissociation of actin bundles and a formation of fine microfilament strands (Fig. 3, G and H). We did not follow the time course in BY-2 cells, but from the findings in coleoptiles (Waller et al., 2002; Holweg et al., 2004), the actin response is completed rapidly in less than 1 h. The debundling of actin might be explained by the upregulation of auxin-responsive ADF genes as previously described in grape (*Vitis vinifera*) stem cuttings (Thomas and Schiefelbein, 2002).

We observed that the synchrony of cell division characterized by elevated frequencies of even-numbered cell files was restored in the YFP-mT line after addition of IAA (Fig. 4D) and, to a lesser extent, of NAA (Fig. 5C). In contrast, additional 2,4-D had no effect on the affected synchrony of cell division in the YFP-mT line.

Several studies have linked the polarity of auxin transport to actin-dependent vesicle flow (for review, see Friml, 2003; Nick, 2006). For instance, the cycling of the auxin-efflux factor PIN1 between intracellular compartments and the plasma membrane could be affected by the actin inhibitor cytochalasin D (Steinmann et al., 1999) or treatment with BFA, a fungal toxin that inhibits the budding of vesicles, results not only in the bundling of cortical actin filaments but also shifts the dose response of auxin-dependent growth toward higher concentrations of auxin (Waller et al., 2002). Conversely, inhibition of myosins by 2,3-butanedione monoxime impairs auxin-dependent cell division in the tobacco cell line VBI-0 (Holweg et al., 2003). The scope of this work was to investigate whether the bundling of actin will impair the polarity of auxin flux monitored by using the synchrony of cell division as a marker.

The experiments by Geldner et al. (2001) have shown that actin is involved in the localization of auxin-efflux factors. Our work extends these observations. It is not only actin per se that is necessary for polar transport of auxin. It is a specific organization of actin that is required. The fine cortical actin filaments observed in the nontransformed cell line are necessary for the patterning of cell division that is dependent on polar auxin flux as to be concluded from the impaired synchrony of cell division in the YFP-mT line and the increased NPA sensitivity of this line. Addition of polar transportable auxin (IAA) but not auxin per se (2,4-D) can restore the fine cortical actin filaments and, in addition, the synchrony in YFP-mT cells, resulting in an ordered pattern of cell divisions where files with even cell numbers are more frequent than files with uneven cell numbers. Thus, the fine cortical actin filaments are sufficient for polar patterning in the background of this cell line. In other words, this study provides evidence for a feedback loop between polar auxin flux and the organization of the actin cytoskeleton. Auxin is therefore able to control its own transport through altering the organization of actin filaments.

CONCLUSION

Future work will focus on two aspects of patterned cell division in BY-2 cells: How is this pattern perpetuated over time, when the number of cells in a file increases progressively? To follow the pattern over time, we will use markers of cell polarity such as PIN1 in conjunction with visualization of actin. When the arrangement of actin filaments is important for pattern formation, then the polarity of actin filaments would decide over patterning via the transport of components necessary for auxin signaling. Although it is not possible to measure auxin efflux in a cell-culture system directly, it might be possible to detect differences in the accumulation of intracellular, radioactively labeled auxin (Petrášek et al., 2003) in the YFP-mT line and the influence of actin recovery after addition of exogenous IAA. To get additional insight into the role of actin organization, we are presently investigating localization and orientation of actin nucleation factors (such as actin-related proteins) during cell division in BY-2 cell files.

MATERIALS AND METHODS

Tobacco Cell Cultures

The tobacco (*Nicotiana tabacum* L. cv BY-2) cell line (Nagata et al., 1992) was cultivated in liquid medium containing 4.3 g/L Murashige and Skoog salts (Duchefa), 30 g/L Suc, 200 mg/L KH_2PO_4, 100 mg/L inositol, 1 mg/L thiamine, and 0.2 mg/L 2,4-D, pH 5.8. Cells were subcultured weekly, inoculating 1.5 to 2 mL of stationary cells into 30 mL of fresh medium in 100-mL Erlenmeyer flasks. The cell suspensions were incubated at 25°C in the dark on an orbital shaker (KS250 basic, IKA Labortechnik) at 150 rpm. Stock BY-2 calli were maintained on media solidified with 0.8% (w/v) agar and subcultured monthly. Transgenic cells and calli were maintained on the same media supplemented with 30 mg/L hygromycin. In some experiments, the cell lines were assessed in the absence of selective pressure but without any differences in patterning. All experiments were performed using cells after 4 d subcultivation.

Transformation and Establishment of Tobacco BY-2 Cells Stably Expressing the YFP-mT Fusion Protein

The *p35S-YFP-mT* construct (Brandizzi et al., 2002) within a binary vector (pVKH18En6) was a kind gift of Dr. Federica Brandizzi (Oxford Brooks University, UK).

For biolistic transformation, gold particles (1.5–3.0 μm; Sigma-Aldrich) were coated with the YFP-mT vector construct according to a modified manual of BIO-RAD (PDS-1000/He Particle Delivery System manual). An amount of 1 μg DNA was used for transfection. DNA-coated gold particles were placed on macrocarriers (BIO-RAD). A cell suspension of 3-d-old BY-2 cells was filtrated onto filter paper. Filtrated BY-2 cells were placed in a particle

gun that was constructed according to Finer et al. (1992) and bombarded by three shots at a pressure of 1.5 bar in the vacuum chamber at −0.8 bar. Following bombardment, which was performed completely under sterile conditions, cells were diluted into liquid medium and kept in the dark at 25°C. After incubation for 24 h, the cells were plated onto solid medium containing 30 mg/L hygromycin. Hygromycin-resistant calli, which appeared after 28 d, were transferred onto new plates and cultured independently until they reached approximately 1 cm in diameter. Cell suspension cultures established from these calli were maintained as described above, with addition of 30 mg/L hygromycin to the cultivation medium. After 6 weeks, a cell line suitable for observing actin filaments was selected by examination of YFP fluorescence by fluorescence microscopy.

Phytotropin and Auxin Treatments

NPA was synthesized by Dr. Wolfgang Michalke (Albert-Ludwigs-Universität Freiburg, Institut für Biologie III, Freiburg, Germany) according to Thompson et al. (1973). NPA and TIBA were added at inoculation from filter-sterilized stocks of 10 mM in dimethyl sulfoxide to final concentrations of 3, 12, or 30 μM. Auxins were also added directly to the final concentration of 2 μM into the standard culture medium using filter-sterilized stocks of 10 mg/mL IAA, 10 mg/mL NAA, and 10 mg/mL 2,4-D dissolved in 96% (v/v) ethanol, respectively. Equal aliquots of sterile dimethyl sulfoxide and ethanol were added to the control samples.

Visualization of Actin Filaments

Actin filaments were visualized by the method of Kakimoto and Shibaoka (1987) modified according to Olyslaegers and Verbelen (1998). Suspended cells were fixed for 10 min in 1.8% (w/v) paraformaldehyde in standard buffer (0.1 M PIPES, pH 7.0, supplemented with 5 mM $MgCl_2$, and 10 mM EGTA). After a subsequent 10-min fixation in standard buffer containing 1% (v/v) glycerol, cells were rinsed twice for 10 min with standard buffer. Then, 0.5 mL of the resuspended cells were incubated for 35 min with 0.5 mL of 0.66 μM TRITC-phalloidin (Sigma-Aldrich) prepared freshly from a 6.6-μM stock solution in 96% (w/v) ethanol by dilution (1:10, v/v) with phosphate-buffered saline (0.15 M NaCl, 2.7 mM KCl, 1.2 mM KH_2PO_4, and 6.5 mM Na_2HPO_4, pH 7.2). Cells were then washed three times for 10 min in phosphate-buffered saline and observed immediately.

For the colocalization experiment of YFP-mT and rhodamine-phalloidin in BY-2 cells overexpressing YFP-mT, the same protocol was used.

Quantification of Pattern and Morphology

From each sample, 0.5-mL aliquots of cells were collected 4 d after inoculation and immediately viewed under an AxioImager Z.1 microscope (Zeiss). Differential interference contrast images were obtained by a digital imaging system (AxioVision; Zeiss) and frequency distributions over the number of cells per individual file were constructed. Cell length and width were also determined from the central section of the cells using the length function of the AxioVision software. Each data point represents 3,000 cell files or cells from three independent experimental series. The results were tested for significance by a *t* test at the 95% confidence level.

Cell viability was analyzed by the Trypan Blue dye exclusion test (Phillips, 1973). Aliquots (0.5 mL) from each sample were stained with 0.4% (w/v) Trypan Blue solution (Sigma-Aldrich) at a ratio of 1:100 (v/v). After incubation for 3 min, the frequency of the unstained (viable) cells was determined as well as the cell number per milliliter using a Fuchs-Rosenthal hematocytometer under bright-field illumination. For each individual sample, 1,000 cells were scored.

For the mitotic indices, 0.5-mL aliquots of cell suspension were fixed in Carnoy fixative (3:1 [v/v] 96% [v/v] ethanol:glacial acetic acid) plus 0.25% Triton X-100 and stained with 2′-(4-hydroxyphenyl)-5-(4-methyl-1-piperazinyl)-2,5′-bi(1H-benzimidazole)-trihydrochloride (Hoechst 33258, Sigma-Aldrich), which was prepared as a 0.5-mg/mL filter-sterilized stock solution in distilled water and used at a final concentration of 1 μg/mL. Cells were recorded under an AxioImager Z.1 microscope (Zeiss) using the filter set 49 4′,6-diamino-phenylindole (excitation at 365 nm, beamsplitter at 395 nm, and emission at 445 nm). The mitotic indices were calculated as the number of cells in mitosis divided by the total number of cells counted. For each time point, 1,000 cells were scored.

Microscopy and Image Analysis

For morphological studies, cells were examined under an AxioImager Z.1 microscope (Zeiss) equipped with an ApoTome microscope slider for optical sectioning and a cooled digital CCD camera (AxioCam MRm). TRITC and YFP fluorescence were observed through the filter sets 43 HE (excitation at 550 nm, beamsplitter at 570 nm, and emission at 605 nm) and 46 HE (excitation at 500 nm, beamsplitter at 515 nm, and emission at 535 nm), respectively (Zeiss). Images were processed and analyzed using the AxioVision (Rel. 4.5) software as described above.

For analysis of division pattern, cells were observed under the same microscope with a 20× objective and differential interference contrast illumination.

Images were processed for publication by the Photoshop software (Adobe Systems).

BY-2 cells were examined under an AxioImager Z.1 microscope (Zeiss) equipped with an ApoTome microscope slider for optical sectioning and a cooled digital CCD camera (AxioCam MRm).

TRITC and RFP fluorescence were observed through the filter set 43 HE (excitation at 550 nm, beamsplitter at 570 nm, and emission at 605 nm). YFP and GFP fluorescence were recorded through the filter sets 46 HE (excitation at 500 nm, beamsplitter at 515 nm, and emission at 535 nm) and 38 HE (Zeiss; excitation at 470 nm, beamsplitter at 495 nm, and emission at 525 nm), respectively, using either a 63× plan apochromat oil-immersion objective or a 40× objective.

Stacks of optical sections were acquired at different step sizes between 0.5 and 0.8 μm. Images were processed and analyzed using the AxioVision software (Rel. 4.5; Zeiss) as described above.

For analysis of division pattern, cells were observed under the same microscope with a 20× objective and differential interference contrast illumination.

For publication, images were processed with respect to contrast and brightness using the Photoshop software (Adobe Systems).

ACKNOWLEDGMENTS

The authors thank Dr. Federica Brandizzi (Oxford Brooks University, UK) for the *p35S-YFP-mT* construct and Sabine Purper (Universität Karlsruhe, Germany) for excellent technical support. NPA was kindly provided by Dr. Wolfgang Michalke (Albert-Ludwigs-Universität Freiburg, Germany).

Received December 3, 2006; accepted February 21, 2007; published March 2, 2007.

LITERATURE CITED

Berleth T, Sachs T (2001) Plant morphogenesis: long-distance coordination and local patterning. Curr Opin Plant Biol **4:** 57–62

Blakeslee JJ, Peer WA, Murphy AS (2005) Auxin transport. Curr Opin Plant Biol **8:** 494–500

Brandizzi F, Snapp EL, Roberts AG, Lippincott-Schwartz J, Hawes C (2002) Membrane protein transport between the endoplasmic reticulum and the Golgi in tobacco leaves is energy dependent but cytoskeleton independent: evidence from selective photobleaching. Plant Cell **14:** 1293–1309

Campanoni P, Blasius B, Nick P (2003) Auxin transport synchronizes the pattern of cell division in a tobacco cell line. Plant Physiol **133:** 1251–1260

Chen R, Masson PH (2006) Auxin transport and recycling of PIN proteins in Plants. *In* J Šamaj, F Baluška, D Menzel, eds, Plant Endocytosis. Springer, Berlin, pp 139–157

Delbarre A, Meller P, Imhoff V, Guern J (1996) Comparison of mechanisms controlling uptake and accumulation of 2,4-dichlorophenoxy acetic acid, naphthalene-1-acetic acid, and indole-3-acetic acid in suspension cultured tobacco cells. Planta **198:** 532–541

Dhonukshe P, Mathur J, Hülskamp M, Gadella TWJ Jr (2005) Microtubule plus-ends reveal essential links between intracellular polarization and localized modulation of endocytosis during division-plane establishment in plant cells. BMC Biol **3:** 11

Finer JJ, Vain P, Jones MW, McMullen MD (1992) Development of the particle inflow gun for DNA delivery to plant cells. Plant Cell Rep **11:** 323–328

Friml J (2003) Auxin transport: shaping the plant. Curr Opin Plant Biol **6:** 7–12

Geldner N, Anders N, Wolters H, Keicher J, Kronberger W, Müller P, Delbarre A, Ueda T, Nakano A, Jürgens G (2003) The *Arabidopsis* GNOM ARF-GEF mediates endosomal recycling, auxin transport, and auxin-dependent plant growth. Cell **112:** 219–230

Geldner N, Friml J, Stierhof YD, Jürgens G, Palme K (2001) Auxin transport inhibitors block PIN1 cycling and vesicle trafficking. Nature **413:** 425–428

Holweg C, Honsel A, Nick P (2003) A myosin inhibitor impairs auxin-induced cell division. Protoplasma **222:** 193–204

Holweg C, Süßlin C, Nick P (2004) Capturing *in vivo* dynamics of the actin cytoskeleton stimulated by auxin or light. Plant Cell Physiol **45:** 855–863

Hou G, Kramer V, Wang Y, Chen R, Perbal G, Gilroy S, Blancaflor E (2004) The promotion of gravitropism in *Arabidopsis* roots upon actin disruption is coupled with the extended alkalization of the columella cytoplasm and a persistent lateral auxin gradient. Plant J **39:** 113–125

Kakimoto T, Shibaoka H (1987) Actin filaments and microtubules in the preprophase band and phragmoplast of tobacco cells. Protoplasma **140:** 151–156

Ketelaar T, Anthony RG, Hussey PJ (2004) Green fluorescent protein-mTalin causes defects in actin organization and cell expansion in Arabidopsis and inhibits actin depolymerizing factor's actin depolymerizing activity in vitro. Plant Physiol **136:** 3990–3998

Kost B, Spielhofer P, Chua NH (1998) A GFP-mouse talin fusion protein labels plant actin filaments *in vivo* and visualizes the actin cytoskeleton in growing pollen tubes. Plant J **16:** 393–401

Leyser O (2006) Dynamic integration of auxin transport and signalling. Curr Biol **16:** 424–433

Lomax TL, Muday GK, Rubery PH (1995) Auxin transport. *In* PJ Davies ed, Plant Hormones: Physiology, Biochemistry, and Molecular Biology. Kluwer, Dordrecht, The Netherlands, pp 509–530

Mattsson J, Sung ZR, Berleth T (1999) Responses of plant vascular systems to auxin transport inhibition. Development **126:** 2979–2991

Morris DA (2000) Transmembrane auxin carrier systems: dynamic regulators of polar auxin transport. Plant Growth Regul **32:** 161–172

Nagata T, Kumagai F (1999) Plant cell biology through the window of the highly synchronized tobacco BY-2 cell line. Methods Cell Sci **21:** 123–127

Nagata T, Nemoto Y, Hasezava S (1992) Tobacco BY-2 cell line as the ''Hela'' cell in the cell biology of higher plants. Int Rev Cytol **132:** 1–30

Nick P (2006) Noise yields order: auxin, actin and polar patterning. Plant Biol **8:** 360–370

Olyslaegers G, Verbelen JP (1998) Improved staining of F-actin and colocalization of mitochondria in plant cells. J Microsc **192:** 73–77

Paciorek T, Zažimalová E, Ruthardt N, Petrášek J, Stierhof YD, Kleine-Vehn J, Morris DA, Emans N, Jürgens G, Geldner N, et al (2005) Auxin inhibits endocytosis and promotes its own efflux from cells. Nature **435:** 1251–1256

Petrášek J, Černá A, Schwarzerová K, Elčkner M, Morris DA, Zažimalová E (2003) Do phytotropins inhibit auxin efflux by impairing vesicle traffic? Plant Physiol **131:** 254–263

Petrášek J, Mravec J, Bouchard R, Blakeslee JJ, Abas M, Seifertová D, Wiśniewska J, Tadele Z, Kubeš M, Čovanová M, et al (2006) PIN proteins perform a rate-limiting function in cellular auxin efflux. Science **312:** 914–918

Phillips HJ (1973) Dye exclusion tests for cell viability. *In* PF Kruse, MK Patterson, eds, Tissue Cultures: Methods and Application. Section VIII: Evaluation of Culture Dynamics. Academic Press, New York, p 406

Redig P, Shaul O, Inze D, Van Montagu M, Van Onckelen H (1996) Levels of endogenous cytokinins, indole-3-acetic acid and abscisic acid during the cell cycle of synchronized tobacco BY-2 cells. FEBS Lett **391:** 175–180

Reinhard D, Mandel T, Kuhlemeier C (2000) Auxin regulates the initiation and radial position of plant lateral organs. Plant Cell **12:** 507–518

Sachs T (1993) The specification of meristematic cell orientation by leaves and by auxin. Aust J Plant Physiol **20:** 541–553

Sachs T (2000) Integrating cellular and organismic aspects of vascular differentiation. Plant Cell Physiol **41:** 649–656

Steinmann T, Geldner N, Grebe M, Mangold S, Jackson CL, Paris S, Gälweiler L, Palme K, Jürgens G (1999) Coordinated polar localization of auxin efflux carrier PIN1 by GNOM ARF GEF. Science **286:** 316–318

Thomas P, Schiefelbein J (2002) Cloning and characterization of an actin depolymerizing factor gene from grape (*Vitis vinifera* L.) expressed during rooting in stem cuttings. Plant Sci **162:** 283–288

Thompson KS, Hertel R, Müller S, Tavares JE (1973) 1-*N*-naphthylphthalamic and 2, 3, 5-triiodobenzoic acids: in vitro binding to particulate cell fractions and action on auxin transport in corn coleoptiles. Planta **109:** 337–352

Waller F, Riemann M, Nick P (2002) A role for actin-driven secretion in auxin-induced growth. Protoplasma **219:** 72–81